Effect of MAF-6 crystal size on its physicochemical and catalytic properties in the cycloaddition of CO_2 to propylene oxide

M.N. Timofeeva[1,2*], I.A. Lukoyanov[1,2], Biswa Nath Bhadra[3],
V.N. Panchenko[1,2], E.Yu. Gerasimov[1], Sung Hwa Jhung[3*]

[1] *Boreskov Institute of Catalysis SB RAS, Prospekt Akad. Lavrentieva 5, 630090, Novosibirsk, Russian Federation*

[2] *Novosibirsk State Technical University, Prospekt K. Marksa 20, 630092, Novosibirsk, Russian Federation*

[3] *Department of Chemistry and Green-Nano Materials Research Center, Kyungpook National University, DaeHak-Ro 80, Buk-Ku, Daegu 41566, Republic of Korea*

Corresponding authors

S.H. Jhung
Tel: +82-53-950-5341
Fax: +82-53-950-6330
E-mail: sung@knu.ac.kr
Address: Department of Chemistry and Green-Nano Materials Research Center, Kyungpook National University, DaeHak-Ro 80, Buk-Ku, Daegu 41566, Republic of Korea

M.N. Timofeeva
Tel.: +7-383-330-7284
Fax: +7-383-330-8056
E-mail: timofeeva@catalysis.ru
Address: Boreskov Institute of Catalysis SB RAS, Prospekt Akad. Lavrentieva 5, 630090, Novosibirsk, Russian Federation

Content

1. Structural properties of ZIFs

Table S1. Structural properties of ZIF-8, MAF-5 and MAF-6 [1]

	ZIF-8	MAF-5 (ZIF-14)	MAF-6 (ZIF-71)
Tightly packed metal imidazolates	$[Zn(Mim)_2]$	$[Zn(Eim)_2]$	$[Zn(Eim)_2]$
Topology	SOD	ANA	RHO
3D framework structure	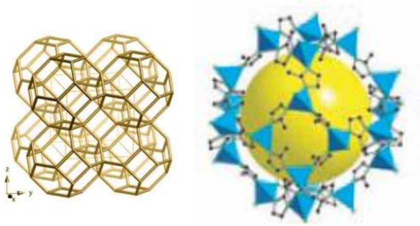	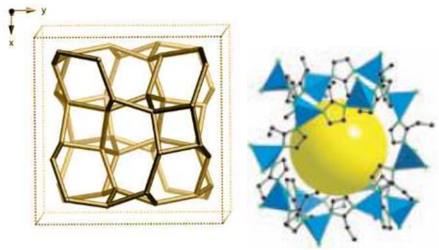	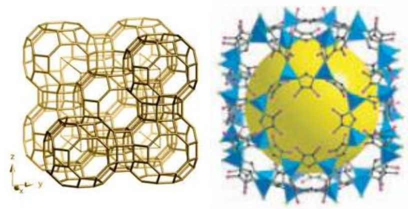
Type of porosity	Cage	Cages	Cages
Cage	$[4^6\,6^8]$	$3\cdot[4^2\,8^2]+2\cdot[6^2\,8^3]$	$3\cdot[4^{12}\,6^8\,8^6]$
Cavity size (Å)	11.6	7x10	18.7
Pore aperture (Å)	3.4x3.4	4.0x5.8	7.6x7.6

2. Characterization of MAF-5

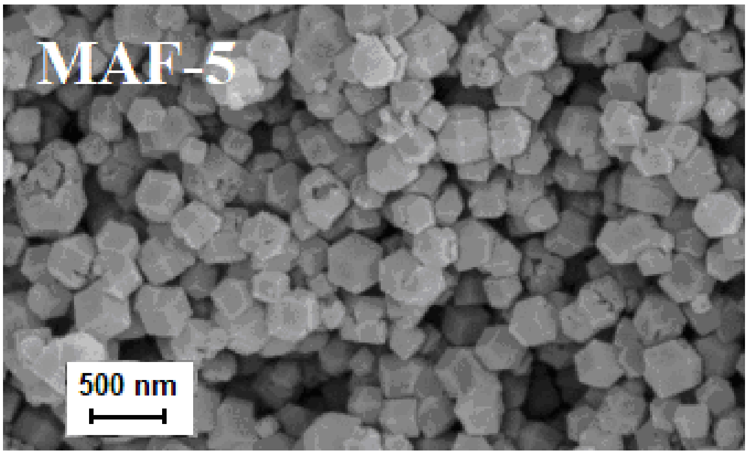

Figure S1. SEM image of MAF-5

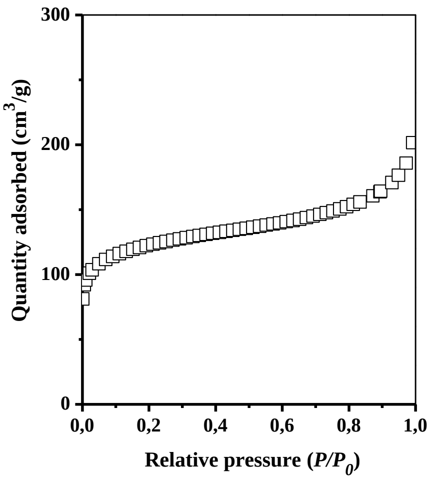

Figure S2. Isotherms of N_2 adsorption-desorption onto MAF-5

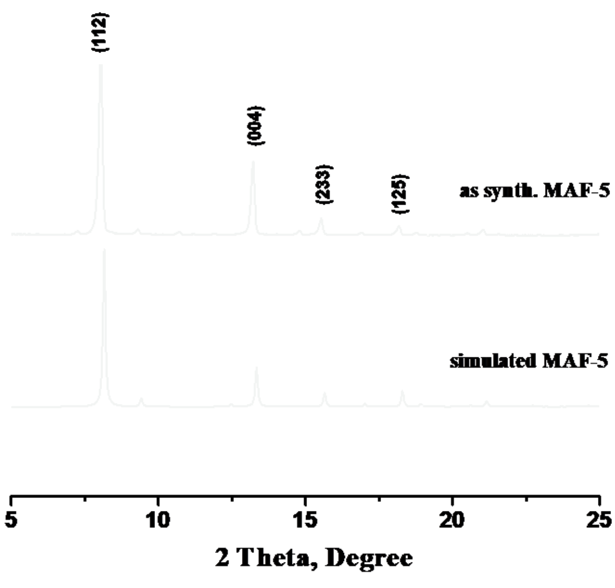

Figure S3. XRD pattern of MAF-5

3. Characterization of MAF-6 samples

3.1. Textural properties of MAF-6 samples

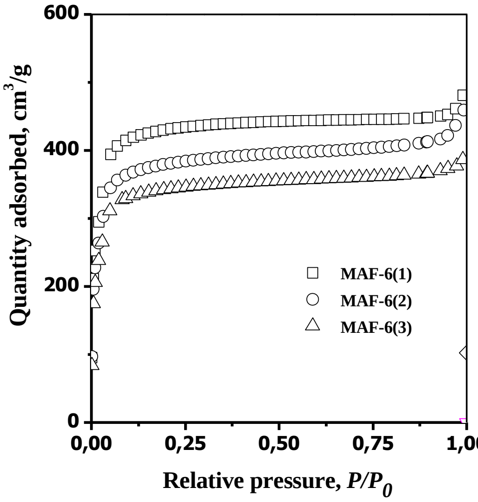

Figure S4. Isotherms of N_2 adsorption-desorption onto MAF-5 and MAF-6 samples

3.1. Characterization of MAF-6 samples by IR spectroscopy

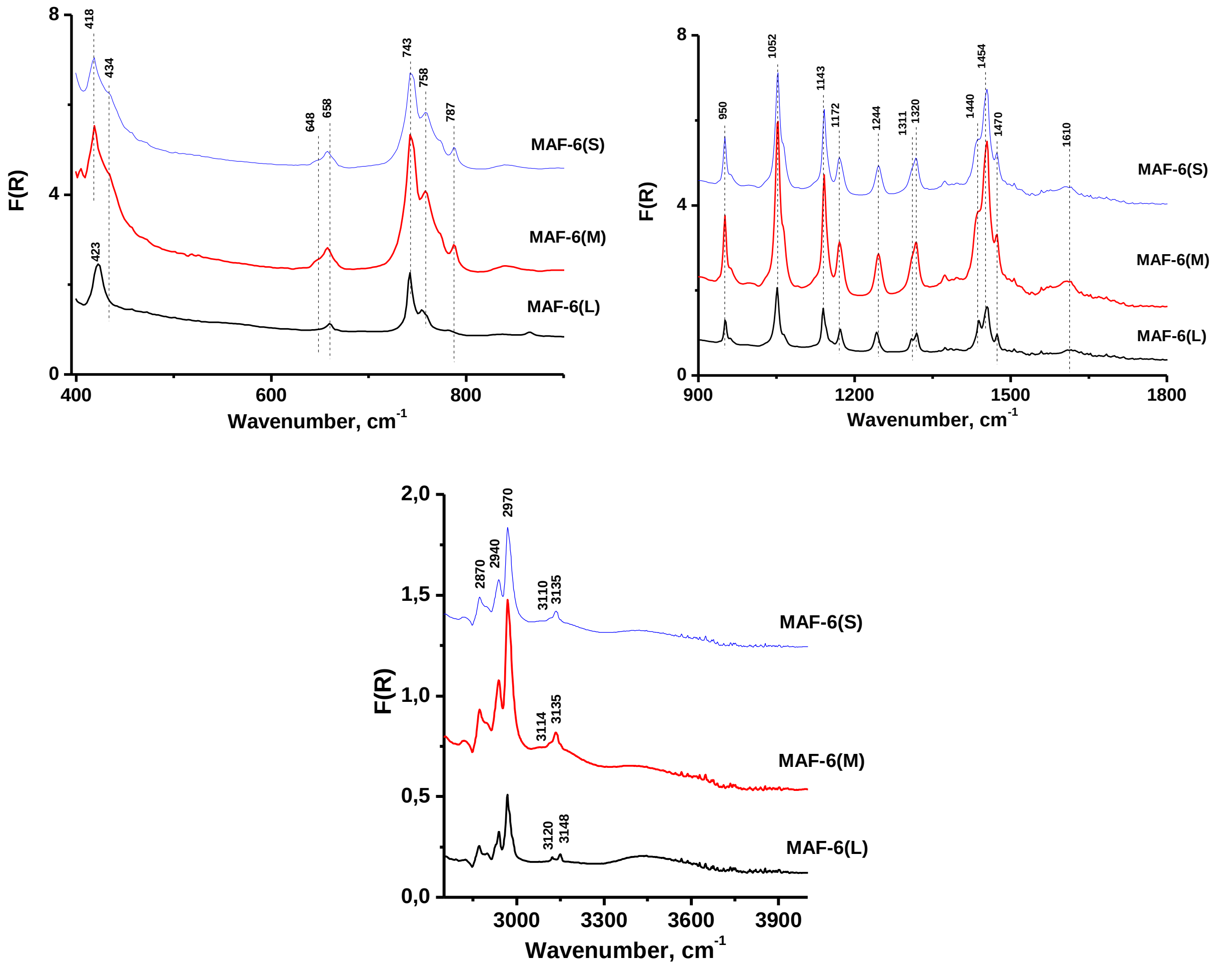

Figure S5. DRIFT spectra of MAF-6 with different particle size

3.3. Characterization of MAF-6 samples by DR-UV-vis spectroscopy

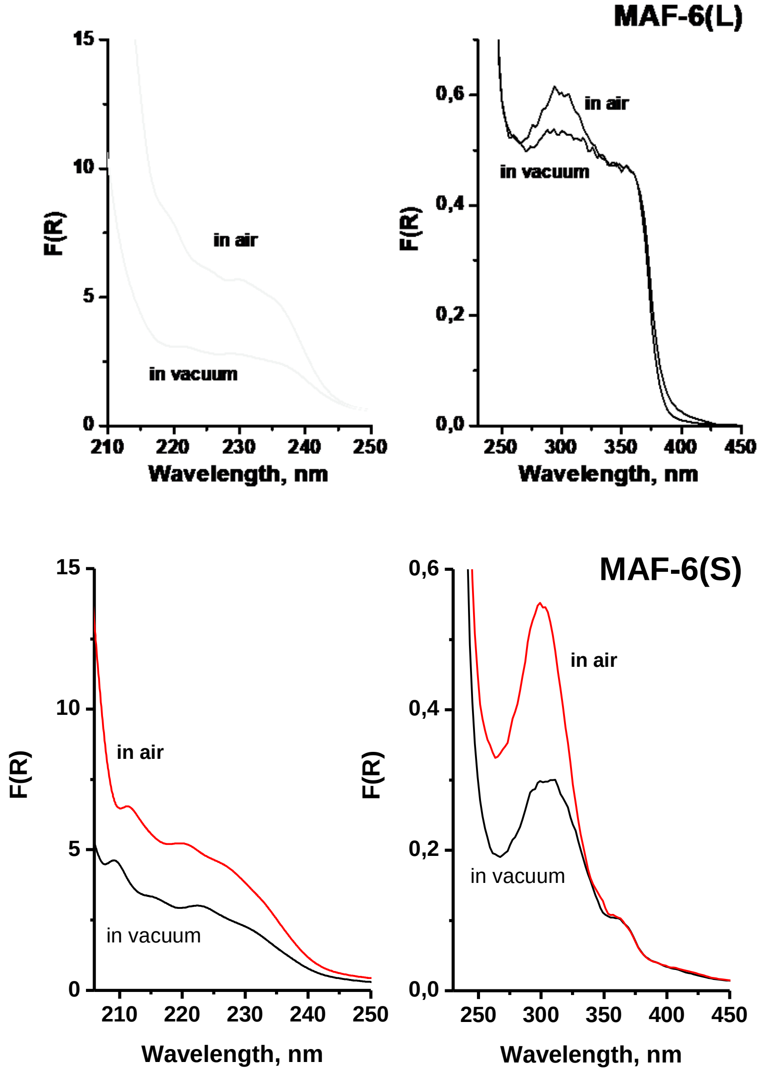

Figure S6. DR-UV-vis spectra of MAF-6(L) and MAF-6(S) after calcination at 150 ^{o}C for 2 h in vacuum and the next addition of wet air

3.4. Characterization of MAF-6 samples by DRIFT spectroscopy using $CDCl_3$ as probe molecule

Sample (0.15-0.2 g) was transferred to a cuvette (cell) suitable for DRIFTS measurements for FTIR characterization. Sample was heated under vacuum at 423 K for 2 h. The strength of the base sites was estimated using the following equation:

$$\log \Delta\nu_{C\text{-}D} = 0.0066\,PA - 4.36 \qquad \text{(Eq. 1)}$$

where $\nu_{C\text{-}D}$ is the shift, in cm^{-1}, of C-D vibration and *PA* is the proton affinity. IR spectra were recorded on a Shimadzu FTIR-8300S spectrometer with a DRS-8000 diffusion reflectance cell in the range between 400 and 6000 cm^{-1} with a resolution of 4 cm^{-1}.

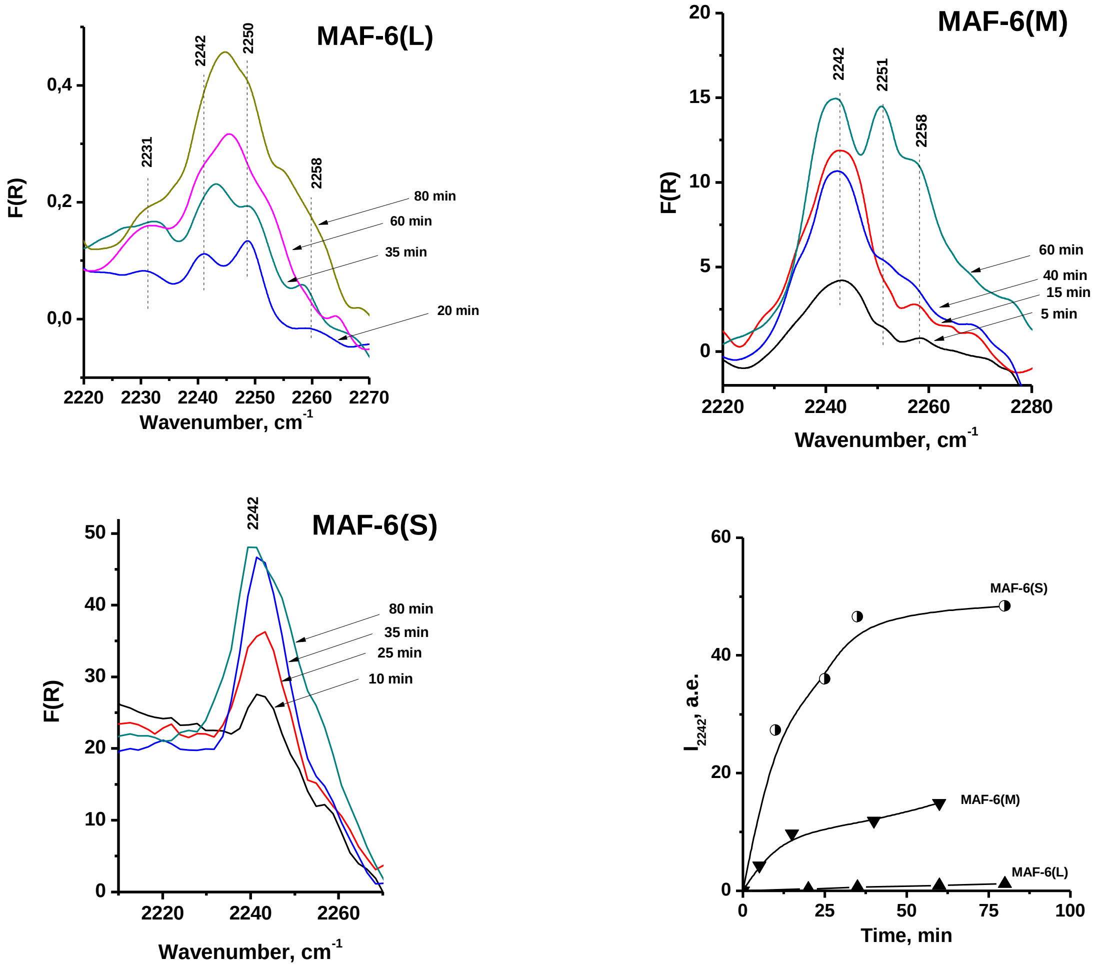

Figure S7. (A-C) DRIFT spectra of $CDCl_3$ adsorbed on MAF-6 samples with different particle size. (D) The change of integral intensity of band at 2242 cm^{-1} in the course of adsorption of $CDCl_3$.

3.5. Characterization of MAF-6 samples by X-ray spectroscopy

Debye-Scherrer's formula (**Eq. 1**) was used to determine the crystal size of MAF-6 [2-3]:

$$D_{XRD} = \frac{0.9 \cdot \lambda}{\beta \cdot \cos\theta} \qquad (1)$$

where D_{XRD} is particle size (nm), β is the full-width at half maximum of the peak (radian), Θ is the Bragg angle of diffraction peak (grad), and λ is *X*-ray wavelength of CuK_{α} (0.1542 nm). The crystal size of MAF-6 was found to change in the order:

MAF-6(L) > MAF-6(M) > MAF-6(S)

It is interesting that reflections shift with increasing crystal size. Thus, the decreasing crystal size from 810 Å to 360 Å leads to shifting reflection of (211) from 7.28° to 7.48° (2θ). Moreover, the intensity of this reflection decreases, and signal half-width broadens. These changes can be related to variation of crystal size

Table S2. MAF-6 particle size estimated from XRD and SEM data

	Particle size			D_{XRD} (Å)	D_{SEM} (Å)	$\frac{D_{SEM}}{D_{XRD}}$
	d_{200}	d_{211}	d_{220}			
MAF-6(L)	38	38	32	36±2	810	23
MAF-6(M)	27	32	27	29±2	360	12
MAF-6(S)	24	24	25	24±1	190	10

4. Catalytic properties

4.1. Catalytic properties of MAF-5

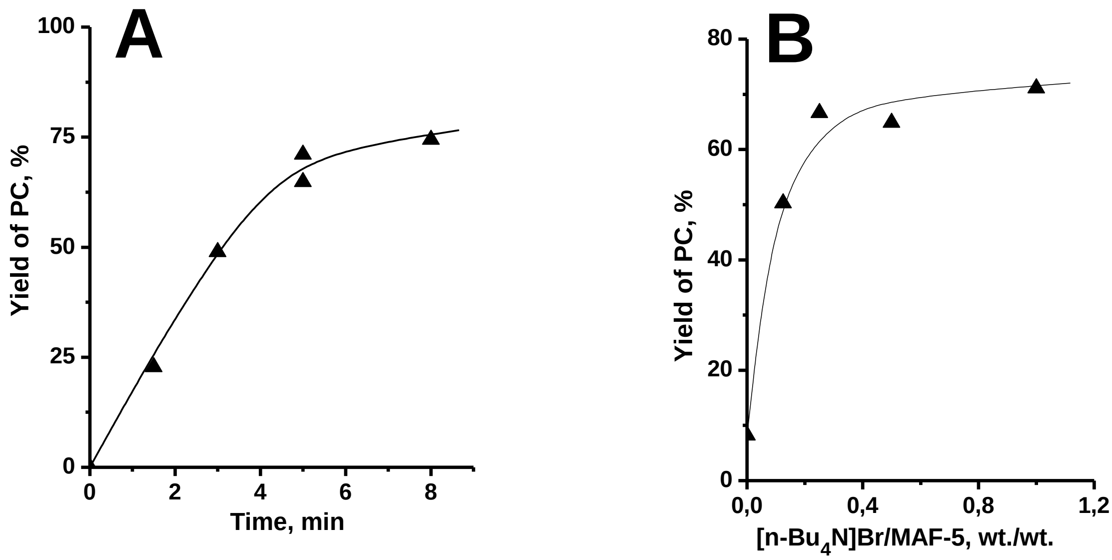

Figure S8. (A) Kinetic curve of propylene carbonate accumulation in the presence of MAF-5 (Experimental conditions: 24 mmol of propylene oxide, 8 atm of CO_2 (at room temperature), 0.85 mmol MAF-5, 0.85 mmol of [n-Bu_4N]Br, 80 ^oC). (B) Effect of [n-Bu_4N]Br amount in reaction mixture on yield of propylene carbonate in the presence of MAF-5 (Experimental conditions: 24 mmol of propylene oxide, 8 atm of CO_2 (at room temperature), 0.85 mmol of catalyst, 80 ^oC, 5 h).

4.2. Catalytic properties of MAF-6 samples

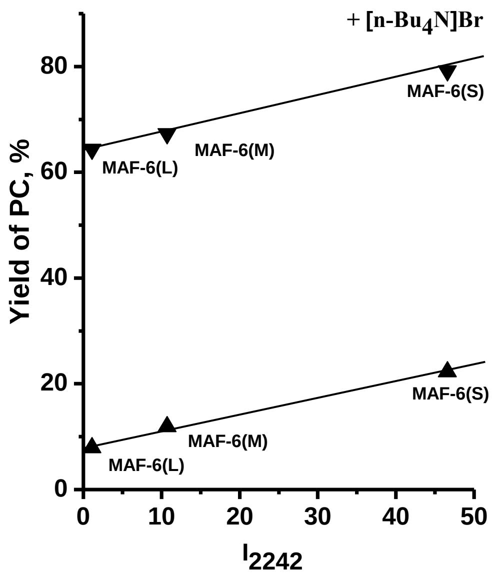

Figure S9. Dependence of PO conversion on the number of basic sites (I_{2242})

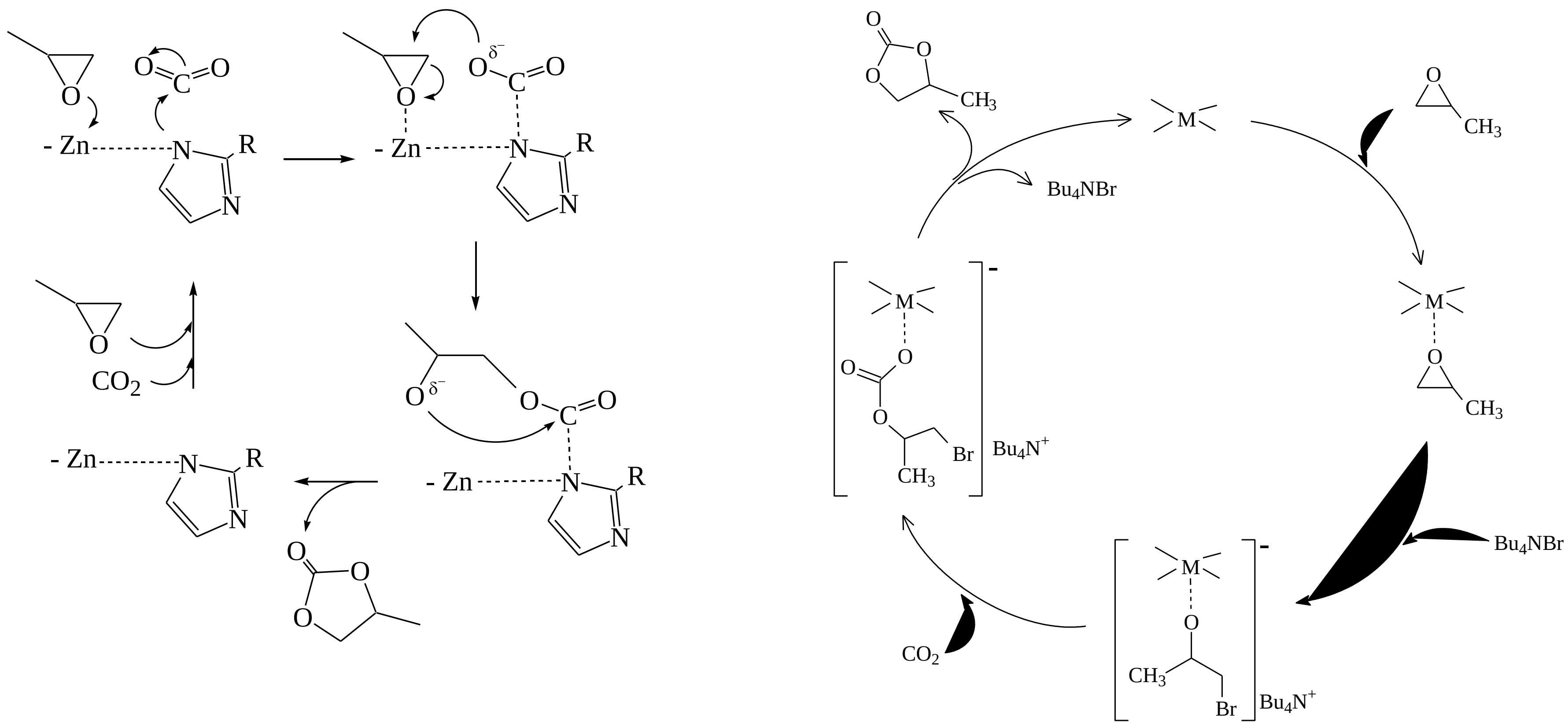

Scheme S1. Mechanisms of reaction between propylene oxide and CO_2

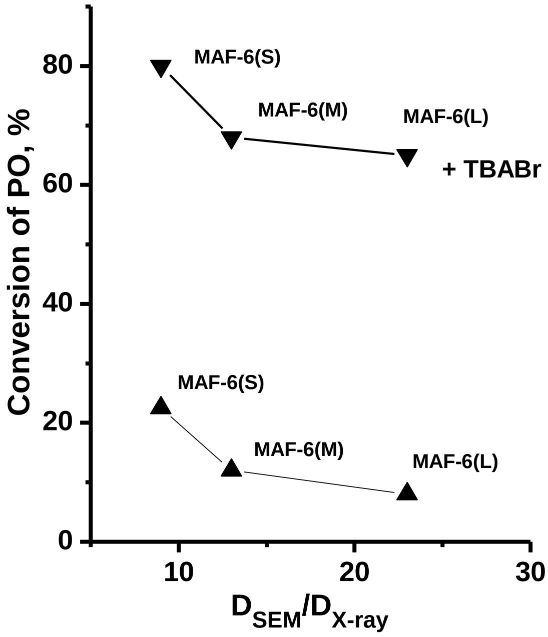

Figure S10. Dependence of PO conversion on the ratio of $D_{SEM}/D_{X\text{-}ray}$.

5. References

[1] Phan, A.; Doonan, C.; Fernando, J.; Uribe-Romo, J.; Knobler, C. B.; O'Keeffe, M.L.; Yaghi O. M., Synthesis, structure, and carbon dioxide capture properties of zeolitic imidazolate frameworks, *Accounts of Chemical Research*, **2010**, 43, 58-67

DOI: 10.1021/ar900116g

[2] Abdel-wahab, M.S.; Jilani, A.; Yahia, I.S.; Al-Ghamdi, A.A.; Enhanced the photocatalytic activity of Ni-doped ZnO thin films: Morphological, optical and XPS analysis, *Superlatt. Microstruct.*, **2016**, 94, 108-118

DOI: 10.1016/j.spmi.2016.03.043

[3] Jilani, A., Abdel-wahab, M. S., Al-ghamdi Attieh A., Dahlan, A. sadik, Yahia, I. S. Nonlinear optical parameters of nanocrystalline AZO thin film measured at different substrate temperatures, *Physica B: Condensed Matter*, **2016**, 481, 97-103

doi:10.1016/j.physb.2015.10.038